

**Synthesis, Characterization, and DNA Interaction Studies of the Ruthenium(II) Complexes  $[\text{Ru}(\text{bpy})_2(\text{ipbp})]^{2+}$  and  $[\text{Ru}(\text{ipbp})(\text{phen})_2]^{2+}$  (ipbp = 3-(1*H*-Imidazo[4,5-*f*][1,10]phenanthrolin-2-yl)-4*H*-1-benzopyran-2-one; bpy = 2,2'-Bipyridine; phen = 1,10-Phenanthroline)**

by Yun-Jun Liu<sup>a)</sup><sup>b)</sup>, Hui Chao<sup>\*a)</sup><sup>c)</sup>, Jun-Hua Yao<sup>d)</sup>, Hong Li<sup>e)</sup>, Yi-Xian Yuan<sup>a)</sup>, Liang-Nian Ji<sup>\*a)</sup><sup>b)</sup>

<sup>a)</sup> Department of Chemistry, Sun Yat-Sen University, Guangzhou 510275, P.R. China  
(fax: 86-20-84035497; e-mail: ceschh@zsu.edu.cn)

<sup>b)</sup> The Key Laboratory of Gene Engineering of Ministry of Education, Sun Yat-Sen University, Guangzhou 510275, P.R. China

<sup>c)</sup> State Key Laboratory of Coordination Chemistry, Nanjing University, Nanjing 210093, P.R. China

<sup>d)</sup> Center of Analysis and Determination, Sun Yat-Sen University, Guangzhou 510275, P.R. China

<sup>e)</sup> Department of Chemistry, Southern China Normal University, Guangzhou 510631, P.R. China

---

A novel ligand 3-(1*H*-imidazo[4,5-*f*][1,10]phenanthrolin-2-yl)-4*H*-1-benzopyran-4-one (ipbp) and its ruthenium(II) complexes  $[\text{Ru}(\text{bpy})_2(\text{ipbp})]^{2+}$  (**1**) and  $[\text{Ru}(\text{ipbp})(\text{phen})_2]^{2+}$  (**2**) (bpy = 2,2'-bipyridine, phen = 1,10-phenanthroline) were synthesized and characterized by elemental analysis and mass, <sup>1</sup>H-NMR, and electronic-absorption spectroscopy. The electrochemical behavior of the complexes was studied by cyclic voltammetry. The DNA-binding behavior of the complexes was investigated by spectroscopic methods and viscosity measurements. The results indicate that complexes **1** and **2** bind with calf-thymus DNA in an intercalative mode. In addition, **1** and **2** promote cleavage of plasmid pBR 322 DNA from the supercoil form I to the open circular form II upon irradiation.

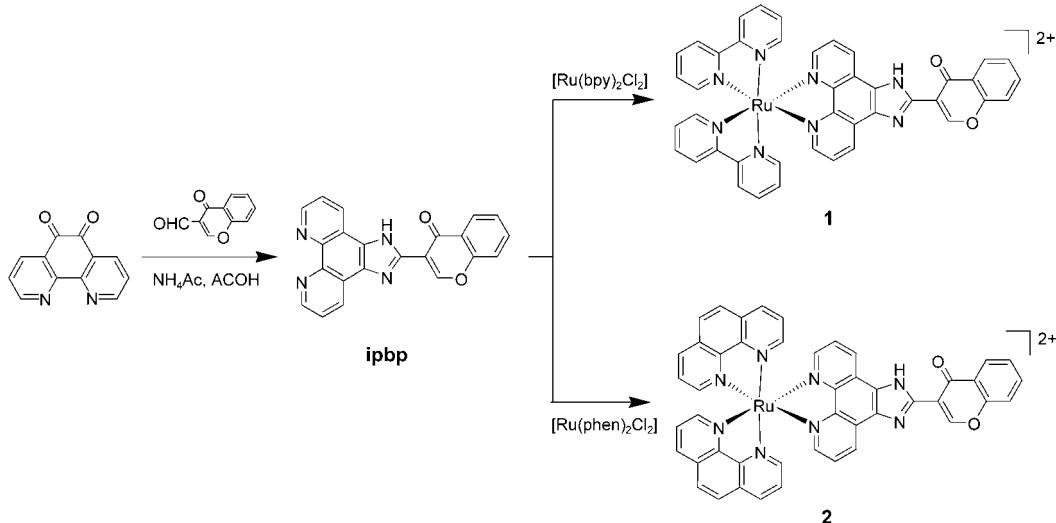
---

**1. Introduction.** – During the past decade, the interaction of transition metal complexes with DNA has received considerable attention due to their potential use in novel probes of nucleic acid structure and new therapeutic reagents [1–3]. Recent studies indicate that (polypyridine)ruthenium(II) complexes ( $[\text{Ru}^{\text{II}}(\text{polypy})]$ ) are promising candidates for DNA structural probe and photocleaving agents because of their rich photochemical properties and varied coordination forms [4–12]. In general,  $[\text{Ru}^{\text{II}}(\text{polypy})]$  complexes can bind DNA in a noncovalent interaction such as electrostatic binding, groove binding, intercalation. Many important applications of these complexes require that the complexes can bind to DNA in an intercalative mode. Therefore, much work has been done on modifying the intercalative ligand. The planarity, aromatic area, and substituting groups of the intercalative ligand have been shown to have effect on the DNA-binding behavior of  $[\text{Ru}^{\text{II}}(\text{polypy})]$  complexes [5]. In our group, much effort has been devoted to the synthesis of new  $[\text{Ru}^{\text{II}}(\text{polypy})]$  complexes and the study of their interaction with DNA [5][13–16]. Based on our previous studies on 2-phenylimidazo[4,5-*f*][1,10]phenanthroline (pip), in which the pip molecule is almost coplanar [14a], we now design a new polypyridine compound 3-(1*H*-imidazo[4,5-*f*][1,10]-phenanthrolin-2-yl)-4-*H*-1-benzopyran-4-one (ipbp) as the intercalative ligand. Some chromenone (=benzopyranone) derivatives are the subject of considerable pharmaceutical and chemical interest [17][18]. The presence of the

chromenone group in ipbp may offer a chance to obtain new interesting photoprobes and photoreagents of DNA. Herein, we report the synthesis and characterization of two novel Ru<sup>II</sup> complexes,  $[\text{Ru}(\text{bpy})_2(\text{ipbp})]^{2+}$  (**1**; bpy = 2,2'-bipyridine) and  $[\text{Ru}(\text{ipbp})(\text{phen})_2]^{2+}$  (**2**; phen = 1,10-phenanthroline). Their interaction with calf-thymus DNA (CT DNA) was explored by spectroscopic methods and viscosity measurements. The abilities of these Ru<sup>II</sup> complexes to induce the cleavage of pBR 322 DNA were also investigated.

**2. Results and Discussion.** – **2.1. Syntheses and Characterization.** For the synthesis of the ligand ipbp (see the *Scheme*), 1,10-phenanthroline-5,6-dione was condensed with 4-oxo-4H-1-benzopyran-3-carboxaldehyde by using a similar method to that described by *Steck and Day* [19]. This method provides a very convenient way to prepare variously aryl-substituted compounds containing an imidazole ring. The mixed-ligand complexes **1** and **2** were prepared by direct reaction of ipbp with the appropriate precursor complexes in ethylene glycol in relatively high yield. The desired Ru<sup>II</sup> complexes were isolated as the perchlorates and purified by column chromatography. In the ES-MS of the complexes, all of the expected signals  $[M-\text{ClO}_4]^{+}$ ,  $[M-2\text{ClO}_4-\text{H}]^{+}$ , and  $[M-2\text{ClO}_4]^{2+}$  were observed. The measured molecular masses were consistent with expected values.

Scheme 1. Preparation of the ipbp Ligand and Ru<sup>II</sup> complexes



The Ru<sup>II</sup> complexes **1** and **2** gave well-defined <sup>1</sup>H-NMR spectra (see *Exper. Part*). The  $\delta(\text{H})$  were assigned by <sup>1</sup>H,<sup>1</sup>H-COSY experiments and by comparison with those of similar complexes [14]. Due to the distinct shielding influences of the adjacent bpy (or phen) and ipbp ligands, the two halves of each bpy (or phen) are not chemically and magnetically equivalent, leading to eight signals corresponding to the bpy (or phen) protons: one set of four was associated with the half of bpy (or phen) near the ipbp, the other set with the half of bpy (or phen) near the other bpy (or phen). Since the

shielding effect of ipbp is obviously more important than that of bpy (or phen), the chemical shifts of the latter protons were larger than those of the former. In addition, the  $\delta(\text{H})$  of H–N of the ipbp imidazole moiety was not observed because this proton exchanged quickly between the two N-atoms of the imidazole ring. A similar example has been reported previously [14a].

The electronic-absorption spectra of the complexes in MeCN were characterized by an intense ligand-centered transition in the UV and a metal-to-ligand charge-transfer (MLCT) transition in the VIS region (see the *Table*). The low-energy absorption bands of **1** and **2** at 458 and 456 nm, respectively, were attributed to the MLCT transition. In the UV region, the intense, fairly sharp bands at 283 nm for **1** and 264 nm for **2** were assigned to the intraligand  $\pi$ - $\pi^*$  transitions by comparison with the spectra of  $[\text{Ru}(\text{bpy})_3]^{2+}$  [20] and  $[\text{Ru}(\text{phen})_3]^{2+}$  [21].

Table 1. *Electrochemical and Absorption Data of the Ruthenium(II) Complexes **1** and **2***

$E_{1/2}/\text{V}$ vs. SCE <sup>a</sup> )		$\lambda_{\text{max}}/\text{nm}^{\text{b}}$ ) ( $\epsilon/\text{dm}^3 \text{ mol}^{-1} \text{ cm}^{-1}$ )		
$\text{Ru}^{\text{II/III}}$	ligand reduction			
<b>1</b>	1.53	–1.17	–1.37	–1.73
<b>2</b>	1.56	–1.20 (irr)	–1.40	–1.73
				458 (4830), 283 (23200), 220 (30000)
				456 (4400), 264 (22600), 225 (17100)

<sup>a</sup>) All complexes were measured in 0.1M  $\text{Bu}_4\text{NClO}_4$ /MeCN, error in potentials was  $\pm 0.02$  V;  $T=23 \pm 1^\circ$ ; scan rate 100 mV·S<sup>–1</sup>. <sup>b</sup>) In MeCN.

**2.2. Molecular-Orbital Calculations.** Extended *Hückel* calculations were carried out to obtain compositions and energies of the ipbp ligand orbitals and to rationalize the electrochemical and spectroscopic results. *Fig. 1* shows the graphical illustrations for the three lowest-lying unoccupied orbitals of ipbp. For these bidentate ligands, we made the following observations: *i*) The lowest vacant molecular orbital is centered at the chromenone part with the electronic distribution. This LUMO is found at  $-9.877$  eV and is thus at a significantly lower energy than the LUMO in isolated bpy ( $-9.767$  eV) and phen ( $-9.717$  eV). *ii*) The next vacant MO, LUMO + 1, lying at higher energy ( $-9.723$  eV) is extended on the phenanthroline-type part, with a strong weight on its N-atoms (coordinating in the complexes). *iii*) In contrast, the next vacant MO, LUMO + 2 ( $-9.302$  eV), is on the phenanthroline-type part with very little electronic density on the chromenone part. This simple electronic approach reflects the nonequivalence of the ipbp ligand. The electronic distribution and orbital energy levels also account for the more pronounced  $\pi$ -acceptor character and the greater energetic stabilization of ipbp with respect to those of the bpy and phen ligands.

**2.3. Electrochemistry.** The electrochemical behavior of complexes **1** and **2** was studied in MeCN by cyclic voltammetry, and the data are summarized in the *Table*. The cyclic voltammograms of **1** and **2** (*Fig. 2*) display well-shaped oxidation (one) and reduction (two or three) waves in the sweep range from  $-2.0$  to  $+2.0$  V. This pattern is common to the most d<sup>6</sup>-metal polypyridine complexes where the redox orbitals are localized on the individual ligands [22]. The anodic and cathodic peak separations vary from 60 to 90 mV and are nearly scan-rate independent, indicating that the processes are reversible one-electron transfers. Complex **1** and **2** exhibit one reversible oxidation at  $+1.53$  and  $+1.56$  V, respectively, which is more positive than that of  $[\text{Ru}(\text{bpy})_3]^{2+}$

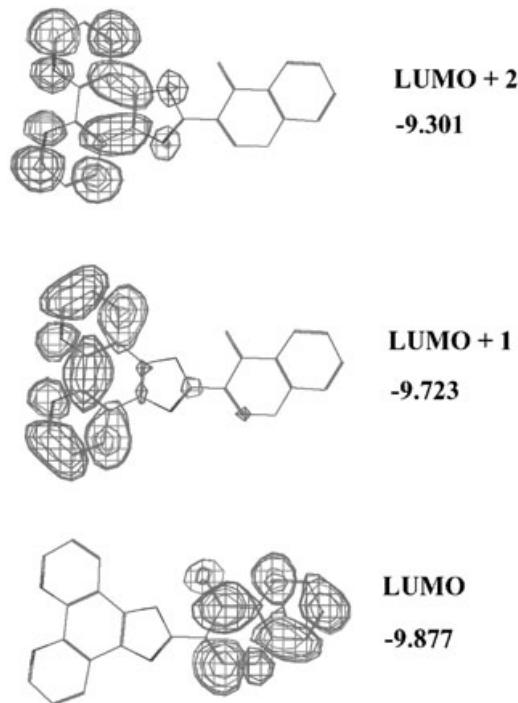


Fig. 1. Graphical illustrations of the three lowest-lying unoccupied orbitals of the ligand ipbp

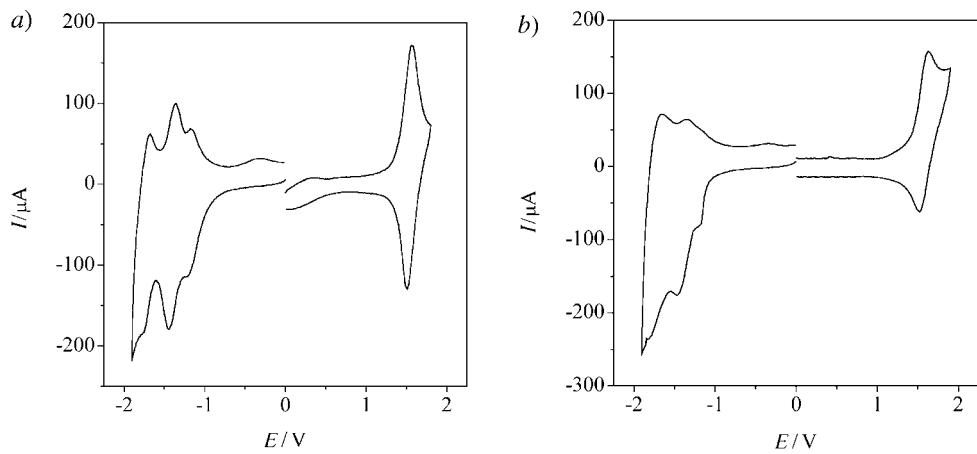
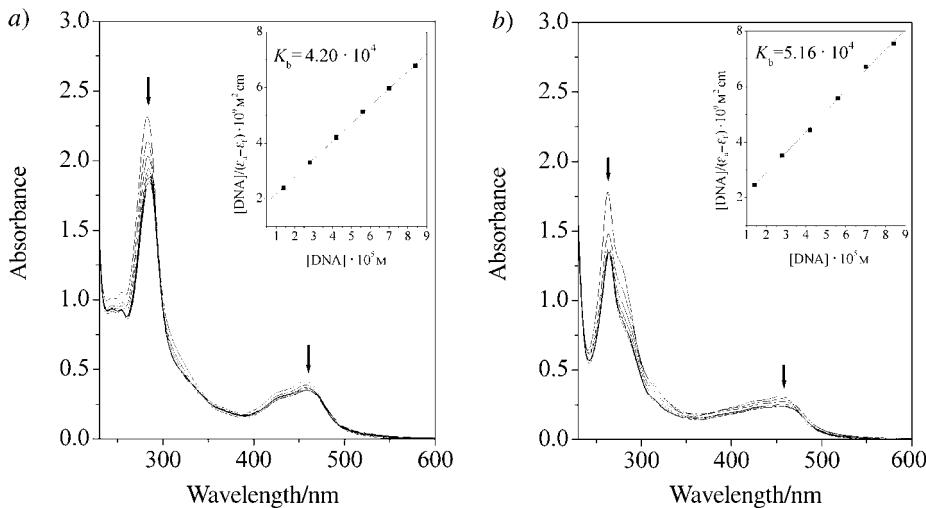


Fig. 2. Cyclic voltammogram of a) complex **1** and b) complex **2** in MeCN

(1.28 V) [23]. This also suggests that the better  $\pi^*$ -acceptor character of the ipbp ligand stabilizes the ruthenium-based HOMO, rendering the oxidation of the metal-ion more difficult.

The two Ru<sup>II</sup> complexes exhibit a number of ligand-based redox couples in the potential range 0 to  $-2.0$  V (vs. SCE); these results can further be rationalized with the molecular-orbital calculations. The first reduction is usually controlled by the ligand having the most-stable lowest unoccupied molecular orbital (LUMO) [24]. As seen in *Fig. 1*, the LUMO is mainly centered on the chromenone portion of ipbp, which is lower in energy than the LUMO of bpy and phen. Thus, the first reductions of **1** ( $-1.17$  V) and **2** ( $-1.20$  V, irr) are assigned to the ipbp ligand. The following two successive reductions are characteristic of the ancillary ligands (bpy or phen) [23][25].

**2.4. DNA-Binding Studies.** **2.4.1. Electronic Absorption Titrations.** In the presence of increasing concentration of calf-thymus DNA, the intraligand and metal-to-ligand (MLCT) transitions of the complexes were significantly perturbed, indicating interaction of the complexes with DNA. *Fig. 3* shows the absorption spectra of complexes **1** and **2** in the presence of increasing amounts of DNA. With increasing DNA concentration, a 3-nm and 2-nm red shift for complexes **1** and **2**, respectively, was found in their MLCT band. The percentage hypochromicity of the MLCT band of **1** and **2** upon binding to DNA was 17.4% and 24.1%, respectively. Comparing with the hypochromism of  $[\text{Ru}(\text{phen})_3]^{2+}$  (12% hypochromism of the MLCT band at 445 nm and a 2-nm red shift) [5a], which interacts with DNA through a semi-intercalation or quasi-intercalation [26], these spectral characteristics obviously suggest that complexes **1** and **2** interact with DNA most likely through a mode that involves a stacking interaction between the aromatic chromophore and the base pairs of DNA.



*Fig. 3.* *Absorption spectra of a) complex **1** and b) complex **2** in Tris·HCl buffer upon addition of CT DNA.  $[\text{Ru}] = 20 \mu\text{M}$ ,  $[\text{DNA}] = 0-100 \mu\text{M}$ . Arrows show the absorbance changing upon the increase of DNA concentration. Insets: Plots of  $[\text{DNA}] / (\epsilon_a - \epsilon_b) \cdot 10^3 \text{ M}^2 \text{ cm}$  vs.  $[\text{DNA}] \cdot 10^3 \text{ M}$  for the titration of DNA with Ru<sup>II</sup> complexes.*

To further illustrate the binding strength of the complexes, the intrinsic binding constant  $K_b$  of **1** and **2** with DNA was determined by monitoring the changes of absorbance in the MLCT band with increasing concentration of DNA. The intrinsic binding constant  $K_b$  of **1** and **2** was  $4.20 \cdot 10^4 \text{ M}^{-1}$  and  $5.16 \cdot 10^4 \text{ M}^{-1}$ , respectively. The

values are comparable to those of so-called DNA-intercalative Ru<sup>II</sup> complexes ( $1.1 \cdot 10^4$ – $4.8 \cdot 10^4 \text{ M}^{-1}$ ) [15a][27] but smaller than that of  $[\text{Ru}(\text{bpy})_2(\text{dppz})]^{2+}$  ( $> 10^6$ ) [28]. The different DNA-binding properties of complexes **1** and **2** are due to the ancillary ligand. On going from bpy to phen, the plane area and hydrophobicity increase, leading to a larger DNA-binding affinity for complex **2**.

**2.4.2. Thermal Denaturation Study.** The thermal behavior of DNA in the presence of complexes can give insight into their conformational changes when the temperature is raised, and offers information about the interaction strength of complexes with DNA. It is well known that on rising the temperature in the solution, the double-stranded DNA gradually dissociates to single strands and generates a hyperchromic effect in the absorption spectra of the DNA bases ( $\lambda_{\text{max}}$  260 nm). To identify this transition process, the melting temperature  $T_m$ , which is defined as the temperature where half of the total base pairs is unbonded, is usually introduced. According to [29–31], the intercalation of natural or synthesized organic compounds and metallointercalators generally results in a considerable increase in  $T_m$ . The thermal denaturation experiment with DNA in the absence of the Ru<sup>II</sup> complexes revealed a  $T_m$  of  $74.8 \pm 0.2^\circ$  under our experimental conditions (Fig. 4). The observed melting temperature in the presence of complexes **1** and **2** were  $81.2 \pm 0.2^\circ$  and  $82.6 \pm 0.2^\circ$ , respectively. These large increases in  $T_m$  ( $\Delta T_m = 6.4^\circ$  and  $7.8^\circ$  for **1** and **2**, resp.) are comparable to those observed for classical intercalators [29–31]. The experimental results also indicated that complex **2** exhibits larger DNA-binding affinity than complex **1** does.

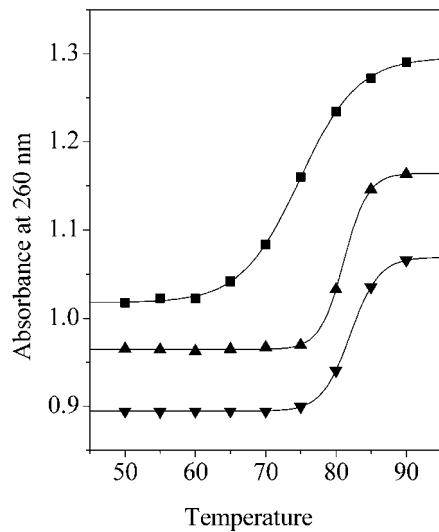


Fig. 4. Thermal denaturation of CT DNA in the absence (■) and presence of complex **1** (▲) and complex **2** (▼).  $[\text{Ru}] = 10 \mu\text{M}$ ,  $[\text{DNA}] = 100 \mu\text{M}$ .

**2.4.3. Fluorescence Spectroscopic Studies.** Complexes **1** and **2** can emit luminescence in Tris buffer at room temperature, with a maximum appearing at 597 and 593 nm, respectively. Thus, a fixed amount (5  $\mu\text{M}$ ) of complex **1** or **2** was titrated with increasing amounts of CT DNA (10–70  $\mu\text{M}$ ). The results of these emission titrations (Fig. 5) showed that upon addition of DNA, the emission intensity of complexes **1** and **2** increased by a factor of 2.52 and 2.76, respectively, as compared to that in the absence

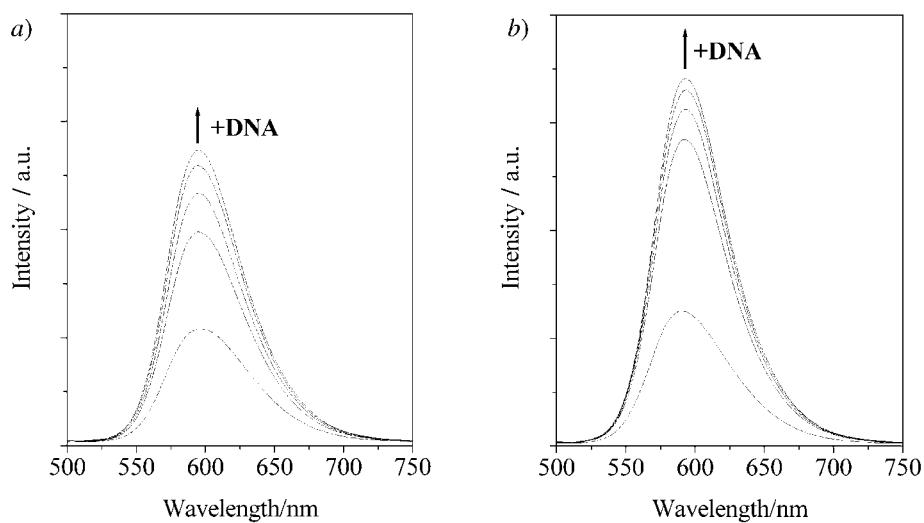


Fig. 5. Emission spectra of a) complex **1** and b) complex **2** in Tris·HCl buffer in the absence and presence of CT DNA. Arrows show the intensity change upon increasing DNA concentration.

of DNA; saturation occurred at a [DNA]/[Ru] ratio of 14. This implies that both complexes can strongly interact with DNA and be protected by DNA efficiently, since the hydrophobic environment inside the DNA helix reduces the accessibility of  $\text{H}_2\text{O}$  solvent molecules to the complex, and the complex mobility is restricted at the binding site, leading to a decrease of the vibrational modes of relaxation.

Fig. 6 shows the steady-state emission-quenching experiments with  $[\text{Fe}(\text{CN})_6]^{4-}$  as quencher. In the absence of DNA, **1** and **2** were efficiently quenched by  $[\text{Fe}(\text{CN})_6]^{4-}$ , resulting in a linear Stern–Volmer plot (slopes 3.43 and 4.61, resp.). In the presence of

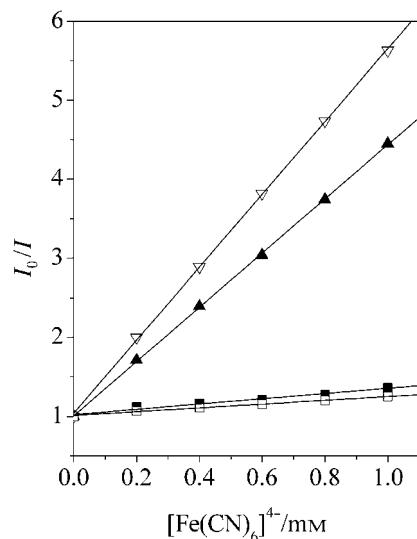


Fig. 6. Emission quenching with  $[\text{Fe}(\text{CN})_6]^{4-}$  for free (▲) or DNA-bound (■) complex **1** and free (▽) or DNA-bound (□) complex **2**.  $[\text{Ru}] = 5 \mu\text{M}$ ,  $[\text{DNA}]/[\text{Ru}] = 40$ .

DNA, however, the slope of the plot (slopes 0.33 and 0.24 for **1** and **2**, resp.) was remarkably decreased. This may be explained by the fact that the bound cations of complexes **1** and **2** are protected from the anionic H<sub>2</sub>O-bound quencher by the array of negative charges along the DNA phosphate backbone [32]. The curvature reflects different degrees of protection or relative accessibility of bound cations. A larger slope for the *Stern – Volmer* curve parallels poorer protection and low binding. Consequently, complex **2** binds to DNA more strongly than complex **1**. This trend is consistent with the observations in the electronic-absorption titration and thermal-denaturation studies.

**2.4.4. Viscosity Measurement.** To further clarify the nature of the interaction between the complexes **1** and **2** and DNA, viscosity measurements were carried out. Optical photophysical probes provide necessary but not sufficient evidence to support the binding model of Ru<sup>II</sup> complexes with DNA. Hydrodynamic measurements that are sensitive to length change (*i.e.* viscosity and sedimentation) are regarded as the least ambiguous and most critical tests of a binding model in soln. in the absence of crystallographic structural data [33][34]. A classical intercalation model demands that the DNA helix lengths as base pairs are separated to accommodate the bound ligand, leading to the increase of DNA viscosity. In contrast, a partial, nonclassical intercalation of ligand could bend (or kink) the DNA helix and reduce its effective length and, concomitantly, its viscosity [33][34]. *Fig. 7* shows the effects of complexes **1** and **2**, together with those of [Ru(bpy)<sub>3</sub>]<sup>2+</sup> and ethidium bromide, on the viscosity of rod-like DNA. Ethidium bromide is well known to bind with DNA through the intercalation mode, while complex [Ru(bpy)<sub>3</sub>]<sup>2+</sup> binds only through the electrostatic mode. No obvious effect of [Ru(bpy)<sub>3</sub>]<sup>2+</sup> on the relative viscosity of the DNA solution was observed. On increasing the amounts of **1** and **2**, the relative viscosity of the DNA solution increased steadily, which is similar to the behavior of ethidium bromide. These results suggest that complexes **1** and **2** intercalate between the base pair of DNA, which is consistent with our foregoing hypothesis.

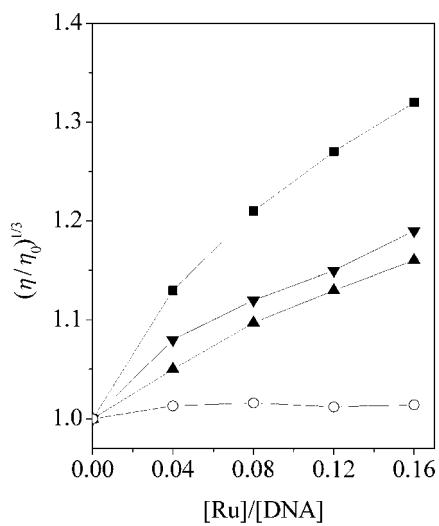
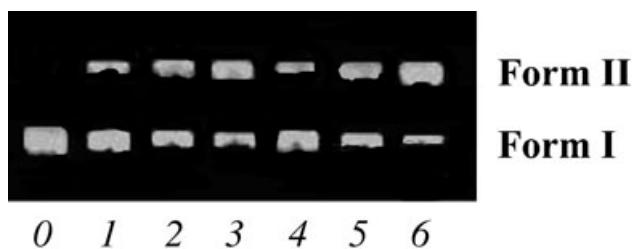


Fig. 7. Effect of increasing amounts of ethidium bromide (■), complex **1** (▲), complex **2** (▼), and [Ru(bpy)<sub>3</sub>]<sup>2+</sup> (○) on the relative viscosity of CT DNA at 28 ± 0.1°. [DNA] = 0.5 mM.

**2.5. Photocleavage of pBR 322 DNA by (Polypyridine)ruthenium(II) Complexes.**

There is substantial and continuing interest in DNA endonucleolytic cleavage reactions that are activated by metal ions [35][36]. The cleavage reaction on plasmid DNA can be monitored by agarose-gel electrophoresis. When circular plasmid DNA is subject to electrophoresis, relatively fast migration will be observed for the intact supercoil form (form I). If scission occurs on one strand (nicking), the supercoil will relax to generate a slower-moving open circular form (form II). If both strands are cleaved, a linear form (form III) that migrates between form I and form II will be generated [37]. *Fig. 8* shows gel-electrophoresis separation of pBR 322 DNA after incubation with the Ru<sup>II</sup> complexes and irradiation at 365 nm. No DNA cleavage was observed for controls in the absence of complexes (*Lane 0*), or after incubation of the plasmid with the Ru<sup>II</sup> complexes in the dark (data not shown). With increasing concentration of the Ru<sup>II</sup> complexes (*Lanes 1–6*), the amount of form I of pBR 322 DNA diminished gradually, whereas that of form II increased. Under comparable experimental conditions, no obvious difference in cleavage activity for complexes **1** and **2** was observed. Although DNA photocleavage by [Ru(phen)<sub>3</sub>]Cl<sub>2</sub> has been reported to involve an <sup>1</sup>O<sub>2</sub>-based mechanism [38], the nature of reactive intermediates involved in the efficient DNA photocleavage by complexes **1** and **2** observed here is not clear. Further detailed studies are currently underway to clarify the cleavage mechanism.



*Fig. 8. Photoactivated cleavage of pBR 322 DNA in the presence of Ru<sup>II</sup> complex: Gel electrophoresis after 60 min irradiation at 365 nm. Lane 0: DNA alone; Lanes 1–3: concentration of complex **1**, 20 (1), 40 (2), and 60  $\mu$ M (3); Lanes 4–6: concentrations of complex **2**, 20 (4), 40 (5), and 60  $\mu$ M (6).*

**3. Conclusion.** – In summary, two novel Ru<sup>II</sup> complexes, [Ru(bpy)<sub>2</sub>(ipbp)]<sup>2+</sup> (**1**) and [Ru(ipbp)(phen)<sub>2</sub>]<sup>2+</sup> (**2**) were synthesized and characterized. Their DNA-binding and photocleavage properties were also investigated. Spectroscopic studies and viscosity experiments indicated that **1** and **2** can intercalate into DNA base pairs *via* the extended chromenone group of the ipbp ligand. When irradiated at 365 nm, two Ru<sup>II</sup> complexes **1** and **2** are efficient photocleavers of the plasmid pBR 322 DNA.

We are grateful to the *National Natural Science Foundation of China*, the *National Science Foundation of Guangdong Province*, the State Key Laboratory of Coordination Chemistry, Nanjing University, and the *Research Fund of Royal Society of Chemistry U.K.* for their financial supports.

#### Experimental Part

*General.* Commercially available materials were used without further purification unless otherwise noted. Doubly distilled H<sub>2</sub>O was used to prepare buffers. Calf-thymus DNA was obtained from the *Sino-American Biotechnology Company*. The 1,10-phenanthroline-5,6-dione [39], *cis*-[Ru(bpy)<sub>2</sub>Cl<sub>2</sub>]·2H<sub>2</sub>O [40], and *cis*-

[Ru(phen)<sub>2</sub>Cl<sub>2</sub>]·2H<sub>2</sub>O [40] were synthesized according to the literature. A soln. of CT DNA in 50 mM NaCl/5 mM Tris (pH 7.2) gave a ratio of UV absorbance at 260 and 280 nm of 1.8–1.9:1, indicating that the DNA was sufficiently free of protein [41]. The DNA concentration per nucleotide was determined by absorption spectroscopy by means of the molar absorption coefficient (6,600 M<sup>-1</sup> cm<sup>-1</sup>) at 260 nm [42]. (Caution: perchlorate complexes are potential explosives that must be handled in small quantity and with great care.) Cyclic voltammetry: CHI 660A electrochemical workstation; purging of the samples with N<sub>2</sub> prior to measurements; standard three-electrode system comprising a Pt-microcylinder working electrode, a Pt-wire auxiliary electrode, and a sat.-calomel reference electrode (SCE). UV/VIS Spectra: Shimadzu MPS-2000 spectrophotometer. Emission spectra: Shimadzu-Rf-2000 luminescence spectrometer; at r.t. <sup>1</sup>H-NMR Spectra: Varian 500 spectrometer;  $\delta$  in ppm rel. to SiMe<sub>4</sub> J in Hz. Fast-atom-bombardment (FAB) MS: VG-ZAB-HS spectrometer; 3-nitrobenzyl alcohol matrix. Electrospray (ESI)MS: LCQ system (Finnigan MAT, USA); MeOH as mobile phase; spray voltage, tube lens offset, capillary voltage, and capillary temp. at 4.50 KV, 30.00 V, 23.00 V, and 200°, resp., *m/z* values for the major peaks in the isotope distribution. Microanalysis (C, H, and N): Perkin-Elmer 240Q elemental analyzer.

**3-(1H-Imidazo[4,5-f][1,10]phenanthrolin-2-yl)-4H-1-benzopyran-4-one (ipbp).** A mixture of 1,10-phenanthroline-5,6-dione (0.315 g, 1.5 mmol), 4-oxo-4H-1-benzopyran-3-carboxaldehyde (0.261 g, 1.5 mmol), NH<sub>4</sub>OAc (2.31 g, 30 mmol), and AcOH (20 ml) was refluxed for 2 h, then cooled to r.t., and diluted with H<sub>2</sub>O (ca. 60 ml). Dropwise addition of conc. aq. ammonia gave a yellow precipitate, which was collected and washed with H<sub>2</sub>O. The crude product in EtOH was purified by filtration through silica gel (60–100 mesh, EtOH). The principal yellow band was collected. On slow evaporation of the soln., a yellow-green solid was obtained, which was dried *in vacuo*: ipbp 70%. FAB-MS: 365 ([M + 1]). Anal. calc. for C<sub>22</sub>H<sub>12</sub>N<sub>4</sub>O<sub>2</sub>: C 72.52, H 3.32, N 15.38; found: C 72.49, H 3.36, N 15.36.

**Bis (2,2'-bipyridine- $\kappa$ N<sup>1</sup>,  $\kappa$ N<sup>1'</sup>)[3-(1H-imidazo[4,5-f][1,10]phenanthrolin-2-yl- $\kappa$ N<sup>1</sup>,  $\kappa$ N<sup>10</sup>)-4H-1-benzopyran-2-one]ruthenium(2+)** Diperchlorate Dihydrate ([Ru(ipbp)<sub>2</sub>(ipbp)](ClO<sub>4</sub>)<sub>2</sub>·2H<sub>2</sub>O; **1**·2ClO<sub>4</sub><sup>-</sup>·2H<sub>2</sub>O). A mixture of *cis*-[Ru(ipbp)<sub>2</sub>Cl<sub>2</sub>]·2H<sub>2</sub>O (0.260 g, 0.5 mmol) and ipbp (0.182 g, 0.5 mmol) in ethylene glycol (20 ml) was heated at 120° under Ar for 6 h (→ clear red soln.). After cooling to r.t., H<sub>2</sub>O (60 ml) was added. After filtration, a red precipitate was obtained by dropwise addition of aq. NaClO<sub>4</sub> soln. The product was purified by column chromatography (alumina, MeCN/toluene 4:1): **1**·2ClO<sub>4</sub><sup>-</sup>·2H<sub>2</sub>O (65%). <sup>1</sup>H-NMR ((CD<sub>3</sub>)<sub>2</sub>SO, arom. region): 9.40 (s, 1 H); 9.10 (d, *J* = 8.5, 2 H); 8.88 (d, *J* = 8.5, 2 H); 8.86 (d, *J* = 8.5, 2 H); 8.35 (d, *J* = 8.5, 1 H); 8.24 (t, *J* = 6, 2 H); 8.12 (t, *J* = 6, 2 H); 8.10 (d, *J* = 8, 2 H); 7.95 (m, 3 H); 7.90 (d, *J* = 8, 1 H); 7.85 (d, *J* = 8, 1 H); 7.68 (m, 2 H); 7.62 (d, *J* = 7, 2 H); 7.61 (t, *J* = 5, 2 H); 7.36 (t, *J* = 5, 2 H). ESI-MS (MeCN): 876 ([M – ClO<sub>4</sub>]<sup>+</sup>), 776.2 ([M – 2ClO<sub>4</sub>H]<sup>+</sup>, 388.6 ([M – 2ClO<sub>4</sub>]<sup>2+</sup>)). Anal. calc. for C<sub>42</sub>H<sub>32</sub>Cl<sub>2</sub>N<sub>8</sub>O<sub>12</sub>Ru: C 49.81, H 3.18, N 11.06; found: C 49.83, H 3.20, N 11.05.

**[3-(1H-Imidazo[4,5-f][1,10]phenanthrolin-2-yl- $\kappa$ N<sup>1</sup>,  $\kappa$ N<sup>10</sup>)-4H-1-benzopyran-2-one]bis(1,10-phenanthroline- $\kappa$ N<sup>1</sup>,  $\kappa$ N<sup>10</sup>)ruthenium(2+)** Diperchlorate Dihydrate ([Ru(ipbp)(phen)<sub>2</sub>](ClO<sub>4</sub>)<sub>2</sub>·2H<sub>2</sub>O; **2**·2ClO<sub>4</sub><sup>-</sup>·2H<sub>2</sub>O). As described for **1**, with *cis*-[Ru(phen)<sub>2</sub>Cl<sub>2</sub>]·2H<sub>2</sub>O (0.284 g, 0.5 mmol): **2**·2ClO<sub>4</sub><sup>-</sup>·2H<sub>2</sub>O (63%). <sup>1</sup>H-NMR ((CD<sub>3</sub>)<sub>2</sub>SO, arom. region): 9.35 (s, 1 H); 9.07 (d, *J* = 8.5, 2 H); 8.78 (d, *J* = 8, 2 H); 8.76 (d, *J* = 8, 2 H); 8.40 (s, 4 H), 8.15 (d, *J* = 4.5, 2 H); 8.10 (d, *J* = 5.5, 2 H); 8.05 (m, 4 H); 7.81 (d, *J* = 7.0, 2 H); 7.73–7.80 (m, 6 H). ESI-MS (MeCN): 925 ([M – ClO<sub>4</sub>]<sup>+</sup>), 824.3 ([M – 2ClO<sub>4</sub>H]<sup>+</sup>), 412.4 ([M – 2ClO<sub>4</sub>]<sup>2+</sup>)). Anal. calc. for C<sub>46</sub>H<sub>32</sub>Cl<sub>2</sub>N<sub>8</sub>O<sub>12</sub>Ru: C 52.08, H 3.04, N 10.56; found: C 52.11, H 3.03, N 10.54.

**Molecular-Orbital Calculations.** The molecular structure of the free ligand ipbp was optimized by the INDO method [43] with the default parameters packaged in the computer program HyperChem, Release 6 (HyperCube, Inc.) [44]. Calculations of the electronic structures were carried out using the extended *Hückel* approximation [45] with the same program by using the default parameters.

**DNA-Binding and -Cleavage Experiments.** The DNA-binding experiments were carried out in Tris buffer solns. (5 mM Tris, 50 mM NaCl, pH 7.2), unless stated otherwise. Stock solns. were stored at 4° and used after no more than 4 days.

The absorption titrations of **1** and **2** in buffer were performed by using a fixed concentration (20  $\mu$ M) of **1** or **2** to which increments of the DNA stock soln. were added. The Ru<sup>II</sup> complex DNA solns. were allowed to incubate for 10 min before the absorption spectra were recorded. The intrinsic binding constants *K*<sub>b</sub> of **1** and **2** to DNA were calculated from *Eqn. 1* [46], where [DNA] is the concentration of DNA in base pairs,  $\epsilon_a$ ,  $\epsilon_f$ , and  $\epsilon_b$  correspond to the apparent absorption coefficient *A*<sub>obsd</sub>/[Ru], the extinction coefficient for the free Ru<sup>II</sup> complex, and the extinction coefficient for the Ru<sup>II</sup> complex in the fully bound form, resp. In plots of [DNA]/( $\epsilon_a$  –  $\epsilon_f$ ) vs. [DNA], *K*<sub>b</sub> is given by the ratio of slope to the intercept.

$$[\text{DNA}] / (\epsilon_a - \epsilon_f) = [\text{DNA}] / (\epsilon_b - \epsilon_f) + 1 / [K_b(\epsilon_b - \epsilon_f)] \quad (1)$$

Thermal denaturation studies were carried out with a *Perkin-Elmer Lambda-35* spectrophotometer equipped with a *Peltier* temperature-controlling programmer ( $\pm 0.1^\circ$ ). The absorbance at 260 nm was continuously monitored for solns. of CT DNA (100  $\mu\text{M}$ ) in the absence and presence of complex (10  $\mu\text{M}$ ). The temperature of the soln. was increased by  $1^\circ \text{ min}^{-1}$ .

For the steady-state emission-quenching experiment with  $[\text{Fe}(\text{CN})_6]^{4-}$  as quencher, the classical *Stern–Volmer* Eqn. 2 [47] was used, where  $I_0$  and  $I$  are the luminescence intensities in the absence and presence of  $[\text{Fe}(\text{CN})_6]^{4-}$ , respectively,  $K$  is a linear *Stern–Volmer* quenching constant depending on the ratio of the bound concentration of  $\text{Ru}^{II}$  complex to the concentration of DNA, and  $r$  is the concentration of the quencher  $[\text{Fe}(\text{CN})_6]^{4-}$ . In the plot of  $I_0/I$  vs.  $r$ , the *Stern–Volmer* quenching constant  $K$  is given by the slope.

$$I_0/I = 1 + K \cdot r \quad (2)$$

Viscosity measurements were carried out with an *Ubbelodhe* viscometer maintained at  $28.0 (\pm 0.1)^\circ$  in a thermostatic bath. DNA Samples with an approximate average length of 200 base pairs were prepared by sonicating to minimize complexities arising from DNA flexibility [48]. Flow time was measured with a digital stopwatch, each sample was measured three times, and an average flow time was calculated. Data were presented as  $(\eta/\eta_0)^{1/3}$  vs. binding ratio [49], where  $\eta$  is the viscosity of DNA in the presence of complex and  $\eta_0$  is the viscosity of DNA alone.

For the gel-electrophoresis experiment, supercoiled pBR 322 DNA (0.1  $\mu\text{g}$ ) was treated with the  $\text{Ru}^{II}$  complex in 50 mM *Tris*·AcOH, 18 mM NaCl buffer pH 7.2. The soln. was then irradiated at r.t. with a UV lamp (365 nm, 10 W). The samples were analyzed by electrophoresis for 1 h at 100 V on a 1% agarose gel in *Tris*·AcOH buffer. The gel was stained with ethidium bromide (1  $\mu\text{g/ml}$ ) and photographed under UV light.

## REFERENCES

- [1] D. M. Perrin, A. Mazumder, D. S. Sigman, in 'Progress in Nucleic Acid Chemistry and Molecular Biology', Vol. 52, Eds. W. Cohn and K. Moldave, Academic Press, New York-Orlando, 1996, p. 123.
- [2] 'Metal Ions in Biological Systems', Eds. A. Sigel and H. Sigel, Vol. 33, Marcel Dekker, New York, 1996.
- [3] K. E. Erkkila, D. T. Odom, J. K. Barton, *Chem. Rev.* **1999**, *99*, 2777.
- [4] I. Ortmans, C. Moucheron, A. Kirsch-De Mesmaeker, *Coord. Chem. Rev.* **1998**, *168*, 233.
- [5] a) Y. Xiong, L. N. Ji, *Coord. Chem. Rev.* **1999**, *185–186*, 711; b) L. N. Ji, X. H. Zou, J. G. Liu, *Coord. Chem. Rev.* **2001**, *216–217*, 513; c) L. N. Ji, Q. L. Zhang, H. Chao, *Chin. Sci. Bull.* **2001**, *461*, 332.
- [6] M. J. Clarke, *Coord. Chem. Rev.* **2003**, *236*, 209.
- [7] J. K. Barton, *Science (Washington, D.C.)* **1986**, *233*, 727.
- [8] A. Ambroise, B. G. Maiya, *Inorg. Chem.* **2000**, *39*, 4256; A. Ambroise, B. G. Maiya, *Inorg. Chem.* **2000**, *39*, 4264.
- [9] E. Tuite, P. Lincoln, B. Nordén, *J. Am. Chem. Soc.* **1997**, *119*, 239; B. Önfelt, P. Lincoln, B. Nordén, *J. Am. Chem. Soc.* **1999**, *121*, 10846; L. M. Wilhelmsson, F. Westerlund, P. Lincoln, B. Nordén, *J. Am. Chem. Soc.* **2002**, *124*, 12092.
- [10] J. G. Collins, J. R. Aldrich-Wright, I. D. Greguric, P. A. Pellegrini, *Inorg. Chem.* **1999**, *38*, 3502; B. T. Patterson, J. G. Collins, F. M. Foley, F. R. Keene, *J. Chem. Soc., Dalton Trans.* **2002**, 4343.
- [11] P. K. L. Fu, P. M. Bradley, D. van Looyen, H. Durr, S. H. Bossmann, C. Turro, *Inorg. Chem.* **2002**, *41*, 3808.
- [12] F. O'Reilly, J. Kelly, A. Kirsch-De Mesmaeker, *J. Chem. Soc., Chem. Commun.* **1996**, 1013; F. M. O'Reilly, J. M. Kelly, *New J. Chem.* **1998**, 215; F. M. O'Reilly, J. M. Kelly, *J. Phys. Chem.* **2000**, *104*, 7206.
- [13] G. Yang, J. Z. Wu, L. Wang, L. N. Ji, X. Tian, *J. Inorg. Biochem.* **1997**, *66*, 171.
- [14] a) J. Z. Wu, B. H. Ye, L. Wang, L. N. Ji, J. Y. Zhou, R. H. Li, Z. Y. Zhou, *J. Chem. Soc., Dalton Trans.* **1997**, 1395; b) J. G. Liu, B. H. Ye, Q. L. Zhang, X. H. Zou, Q. X. Zhen, X. Tian, L. N. Ji, *J. Biol. Inorg. Chem.* **2000**, *5*, 119; c) W. J. Mei, J. Liu, K. C. Zheng, L. J. Lin, H. Chao, A. X. Li, F. C. Yun, L. N. Ji, *J. Chem. Soc., Dalton Trans.* **2003**, 1352; d) H. Xu, K. C. Zheng, H. Deng, L. J. Lin, Q. L. Zhang, L. N. Ji, *New J. Chem.* **2003**, *27*, 1255.
- [15] a) Q. X. Zhen, B. H. Ye, Q. L. Zhang, J. G. Liu, H. Li, L. N. Ji, L. Wang, *J. Inorg. Biochem.* **1999**, *76*, 47; b) X. H. Zou, B. H. Ye, H. Li, Q. L. Zhang, H. Chao, J. G. Liu, L. N. Ji, *J. Biol. Inorg. Chem.* **2000**, *6*, 143; c) H. Deng, J. W. Cai, H. Xu, H. Zhang, L.-N. Ji, *J. Chem. Soc., Dalton Trans.* **2003**, 1.
- [16] H. Chao, G. Yang, G. Q. Xue, H. Li, H. Zhang, I. D. Williams, L. N. Ji, X. M. Chen X. Y. Li, *J. Chem. Soc., Dalton Trans.* **2001**, 1326; H. Chao, W. J. Mei, Q. W. Huang, L. N. Ji, *J. Inorg. Biochem.* **2002**, *92*, 165; C. W.

- Jiang, H. Chao, H. Li, L. N. Ji, *J. Inorg. Biochem.* **2003**, 93, 247; X. L. Hong, H. Chao, L. J. Lin, K. C. Zheng, H. Li, X. L. Wang, F. C. Yun, L. N. Ji, *Helv. Chim. Acta* **2004**, 87, 1180.
- [17] A. Nohara, T. Umetani, Y. Sanno, *Tetrahedron* **1974**, 30, 3553.
- [18] M. Recanatini, A. Bisi, A. Cavall, F. Belluti, S. Gobbi, A. Rampa, P. Valenti, M. Palzer, A. Paluszak, R. W. Hartmann, *J. Med. Chem.* **2001**, 44, 672.
- [19] E. A. Steck, A. R. Day, *J. Am. Chem. Soc.* **1943**, 65, 452.
- [20] G. M. Bryant, J. E. Fergusson, H. K. J. Powell, *Aust. J. Chem.* **1971**, 24, 257.
- [21] A. T. Cocks, R. D. Wright, K. R. Seddon, *Chem. Phys. Lett.* **1982**, 85, 369.
- [22] B. K. Ghosh, A. Chakravorty, *Coord. Chem. Rev.* **1989**, 95, 239.
- [23] A. Kirsch-De Mesmaeker, R. Nasielski-Hinkens, D. Maetens, D. Pauwels, J. Nasielski, *Inorg. Chem.* **1984**, 23, 377.
- [24] J. E. B. Johnson, R. R. Ruminski, *Inorg. Chim. Acta* **1993**, 208, 231.
- [25] F. Barigelli, A. Juris, A. Balzani, P. Belser, A. von Zelewsky, *Inorg. Chem.* **1987**, 26, 4115.
- [26] P. Lincoln, B. Nordén, *J. Phys. Chem. B* **1998**, 102, 9583.
- [27] A. M. Pyle, J. P. Rehmann, R. Meshoyer, C. V. Kumar, N. J. Turro, J. K. Barton, *J. Am. Chem. Soc.* **1989**, 111, 3051.
- [28] J. E. Coury, J. R. Anderson, L. McFail-Isom, L. D. Williams, L. A. Bottomley, *J. Am. Chem. Soc.* **1997**, 119, 3792.
- [29] M. J. Waring, *J. Mol. Biol.* **1965**, 13, 269.
- [30] J. M. Kelly, A. B. Tossi, D. J. McConell, C. OhUigin, *Nucleic Acids Res.* **1985**, 13, 6017.
- [31] G. A. Neyhart, N. Grover, S. R. Smith, W. A. Kalsbeck, T. A. Fairly, M. Cory, H. H. Thorp, *J. Am. Chem. Soc.* **1993**, 115, 4423.
- [32] C. V. Kumar, N. J. Turro, J. K. Barton, *J. Am. Chem. Soc.* **1985**, 107, 5518.
- [33] S. Satyanarayana, J. C. Dabrowiak, J. B. Chaires, *Biochemistry* **1992**, 31, 9319.
- [34] S. Satyanarayana, J. C. Dabrowiak, J. B. Chaires, *Biochemistry* **1993**, 32, 2573.
- [35] D. S. Sigman, *Acc. Chem. Res.* **1986**, 19, 180.
- [36] S. Sitolani, E. C. Long, A. M. Pyle, J. K. Barton, *J. Am. Chem. Soc.* **1992**, 114, 2303.
- [37] J. K. Barton, A. L. Raphael, *J. Am. Chem. Soc.* **1984**, 106, 2466.
- [38] H. Y. Mei, J. K. Barton, *Proc. Natl. Acad. Sci. U.S.A.* **1988**, 85, 1339.
- [39] M. Yamada, Y. Tanaka, Y. Yoshimato, S. Kuroda, I. Shimao, *Bull. Chem. Soc. Jpn.* **1992**, 65, 1006.
- [40] B. P. Sullivan, D. J. Salmon, T. J. Meyer, *Inorg. Chem.* **1978**, 17, 3334.
- [41] J. Marmur, *J. Mol. Biol.* **1961**, 3, 208.
- [42] M. F. Reichmann, S. A. Rice, C. A. Thomas, P. Doty, *J. Am. Chem. Soc.* **1954**, 76, 3047.
- [43] J. N. Murrell, A. J. Harget, 'Semi-empirical Self-consistent-field Molecular Orbital Theory of Molecules', Wiley Interscience, New York, 1971.
- [44] 'Hyperchem', Release 6.01 for Windows, Hypercube Inc., 2000.
- [45] R. Hoffmann, *J. Chem. Phys.* **1963**, 39, 1397.
- [46] A. Wolf, G. H. Shimer Jr., T. Meehan, *Biochemistry* **1987**, 26, 6392.
- [47] J. R. Lakowicz, G. Webber, *Biochemistry* **1973**, 12, 4161.
- [48] J. B. Chaires, N. Dattagupta, D. M. Crothers, *Biochemistry* **1982**, 21, 3933.
- [49] G. Cohen, H. Eisenberg, *Biopolymers* **1969**, 8, 45.

Received August 11, 2004